Heterogeneous & Homogeneous & Bio- & Nano-

CHEMCATCHEM

CATALYSIS

Title: Spirobifluorene-based porous organic polymers as efficient porous support for Pd and Pt for the selective hydrogenations

Authors: Mihaela Trandafir, Lidia Pop, Niculina Daniela Hadade, Ioana Hristea, Cristian Mihail Teodorescu, Frank Krumeich, Jeroen Anton van Bokhoven, Ion Grosu, and Vasile I. Parvulescu

To be cited as: *ChemCatChem* 10.1002/cctc.201801247

Link to VoR: http://dx.doi.org/10.1002/cctc.201801247

A Journal of ChemPubSoc Europe

WILEY-VCH

www.chemcatchem.org

10.1002/cctc.201801247

Spirobifluorene-based porous organic polymers as efficient porous support for Pd and Pt for the selective hydrogenations

Mihaela Trandafir[a]#, Lidia Pop[b] #, Niculina D. Hădade[b], Ioana Hristea[c], Cristian Mihail Teodorescu[c], Frank Krumeich[d], J.A. van Bokhoven[d] *, Ion Grosu[b]* and Vasile I. Parvulescu[a]*

[a]University of Bucharest, Department of Organic Chemistry, Biochemistry and Catalysis, 4-12 Regina Elisabeta Blvd., 030016 Bucharest, Romania; E-mail: vasile.parvulescu@chimie.unibuc.ro

[b]Babes-Bolyai University, Faculty of Chemistry and Chemical Engineering, Department of Chemistry, Cluj-Napoca, 11 Arany Janos str., 400028, Cluj-Napoca, Romania, e-mail: igrosu@chem.ubbcluj.ro

[c]National Institute of Materials Physics, Department of Surfaces and Interfaces, Atomistilor 405 A, 077125 Magurele-Ilfov, Romania, e-mail: teodorescu@infim.ro

[d] Institute for Chemical and Bioengineering, ETH Zurich, HCI D 130 Vladimir-PrelogWeg 1, 8093 Zurich, Switzerland, Paul Scherrer Institure, 5323 Villigen, Switzerland, e-mail: jeroen.vanbokhoven@chem.ethz.ch

#- participated equally

Spirobifluorene-based porous organic polymers (POP) were synthesized following two different protocols; the acetylenic coupling reaction conditions and the Sonogashira cross-coupling reaction. These were utilized as support for the hydrogenation of a series of species containing unsaturated C=C and C=O bonds (4-nitrostyrene, 4-bromobenzophenone, acetophenone, 7-nitro-1-tetralone and 1,2-naphtoquinone confirmed their efficiency). POP1 prepared via a copper-catalysis protocol was completely inactive, while POP2-4 containing residual Pd exhibited different activities in accordance to the accessibility of the substrates to the metal. Further deposition of 0.5wt% Pd led to active and stable catalysts. They were easily separated by filtration, and after re-dispersion, afforded the same performances for ten successive cycles. This study also evidenced the specific role of the support in these reactions by comparing the behaviour of Pd/POP with that of a Pd/C catalyst with the same loading of palladium. The deposition of Pt on these supports led to sub-nanometric particles and, in accordance, to a different catalytic behaviour reflected merely by differences in the selectivity.

Introduction

The chemoselective reduction of organic compounds is an important step in the synthesis of various valuable compounds for both industrial and fine chemical processes.[1] Among others, the selective hydrogenation of the carbonyl compounds to the corresponding alcohols may produce platform molecules for the synthesis of different fine-chemicals.[2] Literature has largely investigated this reaction taking as substrates both aldehydes and ketones and molecular hydrogen or isopropanol as the hydrogen source.[3]

Hydrogenation by molecular hydrogen requires an adequate catalyst able to dissociate the hydrogen and to activate the substrate. Generally, the catalysts used for the reduction reactions contain transition metals (Fe, Co, Ni, Cu, Ru, Rh, Pd, Ir, Pt, Au).[4, 5] Further heterogenization of these catalysts by their deposition onto solid supports, especially as metal nanoparticles (NPs), provides specific advantages as high turnover number (TON), good selectivity and good recyclability.[6] An adequate support eliminates some drawbacks, as the agglomeration during their synthesis or reaction. The use of porous supports with a high surface area and controlled pore size distribution allows an increased productivity and shape control selectivity.[7]

Metal oxide catalysts can act as appropriate supports, some of them being also active for hydrogen transfer reactions.[8] They afford large surface areas, have a very good dispersion of the catalytic active phase and may influence the oxidation state of the metal and ensure hydrogen to spillover.[9] Materials such as mesoporous activated carbon, graphitic carbon nitride, carbon nanotubes and graphenes are also suitable supports for the metal catalysts in the hydrogenation reactions.[10] These materials have the advantage of sustainability, as these can be produced from renewable resources.

Among these, porous organic polymers (POPs) gained a significant interest, the very large surface areas and the good thermal stability recommending them as adsorbents and catalytic supports.[11] The intrinsic properties of these new materials are the effect of the covalent organic bonds participating in their construction,[12] while the catalytic ones are afforded by isolated ions,[13] entrapped metal-complexes or nanoparticles.[14] The porous structure is able to stabilize the metal NPs, making these highly active and reusable for heterogeneous catalysis.[15]. In this context POP supported palladium catalysts showed efficiency for controlling the selectivity in specific reactions as Suzuki–Miyaura, Heck, and Sonogashira cross-couplings [16], or the chemoselective decarbonylation of aldehydes[17].

In comparison to the coordination-bonded MOFs, POPs are generally less susceptible to chemical degradation and water. This ensures the intactness of the catalysts during operation. Both the structure and texture of these porous materials can be intimately tailored by the selection of the building units.[18] In this way, these materials may enhance the properties of the carbonaceous supports.[19] They can be constructed through covalent bonds, such as C–C ones[20] from a variety of building blocks, including tetrahedral units starting from derivatives of tetraphenyl-methane,[21-24] -silane,[23-25] -adamantane[21, 24, 26, 27] or 9,9'-spirobifluorene.[28] Today, the synthesis of POPs can be done using different building blocks from very simple ones, such as benzene (in Friedel-Crafts reaction with $CH_2(OMe)_2$),[29] to more elaborated structures, such as compounds with tetrahedral geometry (e.g. tetrakis(*p*-substituted-phenyl)methane,[22, 27] tetrakis(*p*-substituted-phenyl)silane[25] or tetrakis(*p*-substituted-phenyl)adamantane[27]). Assembling strategies include Suzuki,[30] Sonogashira,[31] and Yamamoto,[21, 28, 32] cross-couplings, and boroxine[33] and imine[34] synthesis reactions.[35]

Compared to metal organic frameworks (MOFs), POPs are considerably more robust. Their stability is ensured by connections made by covalent bonds instead of the chemically susceptible coordination bonds of MOFs. Salient functionalities can also be integrated via covalent bonds. Examples are basic N-heterocycles,[36] acidic motifs[37] and chiral entities.[23, 38]

Based on this state of the art, this study aimed the synthesis and characterization of new polymer organic frameworks, using a tetrahedral substrate exhibiting 3,3',6,6'-tetrasubstituted-spirobifluorene units (Scheme 1). They were coupled using either the Sonogashira protocol or acetylenic coupling reactions. The resulted polymers were used as support for Pd to produce new selective and reusable catalysts for the hydrogenation of several ketones (acetophenone(ACP), 4-bromobenzophenone (4-BBP), 1,2-naphtoquinone (1,2-NQ) and 7-nitro-1-tetralone (7N-1T)). An aromatic nitro compound (4-nitrostyrene (4-NS)) has also been hydrogenated in these experiments. The challenge using aromatic ketones as substrates is that it is more difficult to selectively hydrogenate the carbonyl group due to the strong positive electromer effect (+E) induced by the presence of the aromatic group.

The new organic polymers take advantage of remnant Pd from the Sonogashira synthesis. The additional loading of Pd was 0.5 wt.%. The resulted materials were exhaustively characterized.

Results and Discussion

Synthesis of the porous organic polymers

The synthesis of key compounds (**4** and **6**) for the access to POP’s followed a strategy developed in our group starting from the parent spiro compound **1** (Scheme 1).[39]

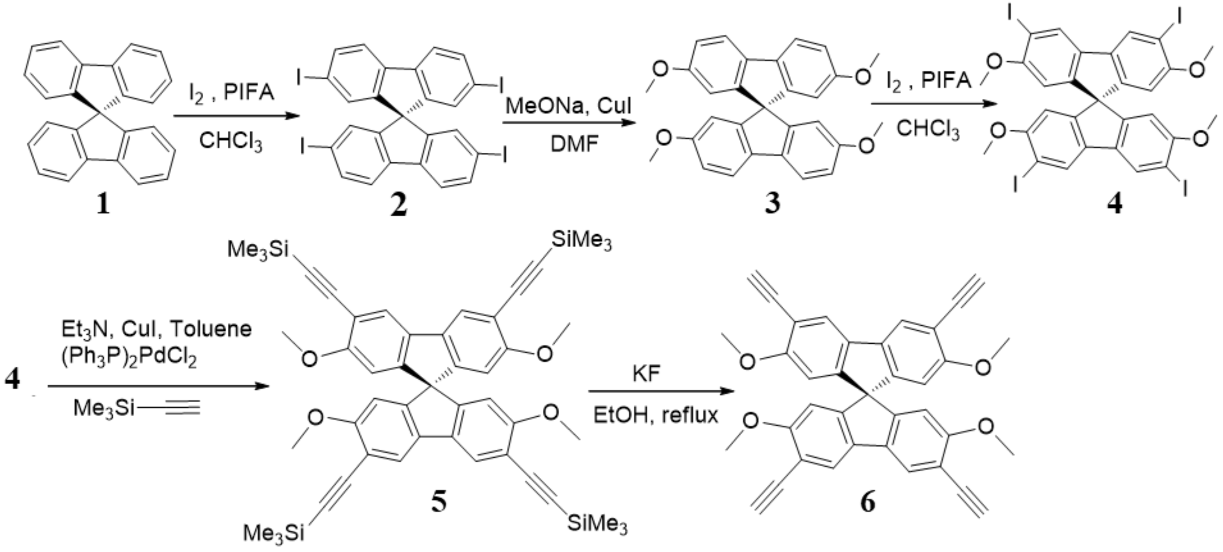

Scheme 1

The POPs with tetrasubstituted-9,9’-spirobifluorene motif exhibit different geometries according to the positions of the reactive groups in the starting 9,9’spirobifluorene derivative. The substituents located at positions 2,2',7,7', as it is the case in the most common derivatives, lead to macromolecules with a planar structure, with perpendicular growing axes that are disposed in close parallel planes, which delimit a thin sheet (Scheme 1). Substituents located at the positions 3,3',6,6' yield tetrahedral growing axes, as in tetrakis(*p*-substituted-phenyl)-methane and adamantane (Scheme 2). A correction of the geometry and the synthesis of tetrahedral POPs with derivatives of type I (having the substituents at positions 2,2’,7,7’) can be done if this substrate reacts with reagents exhibiting an appropriate geometry, such as *meta*-di-substituted benzene.

Scheme 2

Catalysts characterization

The investigated POP1-4 shown a good thermal stability. Except POP1, which starts to decompose at 200 °C, all other catalysts decompose above 250 °C (Figure SI1). As the DTA profiles demonstrated, the decomposition of these materials occurs in successive steps, specific for each polymer (Figure SI1).

The adsorption-desorption isotherms of N_2 at -196 °C of POP1-4 and the corresponding Pd- or Pt/POP2 catalysts exhibit a type IV shape (Figure SI2) with a H4 type hysteresis loop, often associated with mesoporous slit-like pores. The deposition of the noble metals (0.5wt% Pd or Pt) onto POP2 did not alter the shape of the adsorption-desorption isotherms but produced a decrease of the surface (BET and Langmuir) areas and with very small changes in the pore size (Figure SI3). These results confirm that i) the structure/texture of the polymer is not affected by the deposition-precipitation process and ii) the metals do not agglomerate to block the pores. However, for Pt, the decrease of the surface area and the pore size was more evident than for Pd which may suggest it is merely located at the pore mouth.

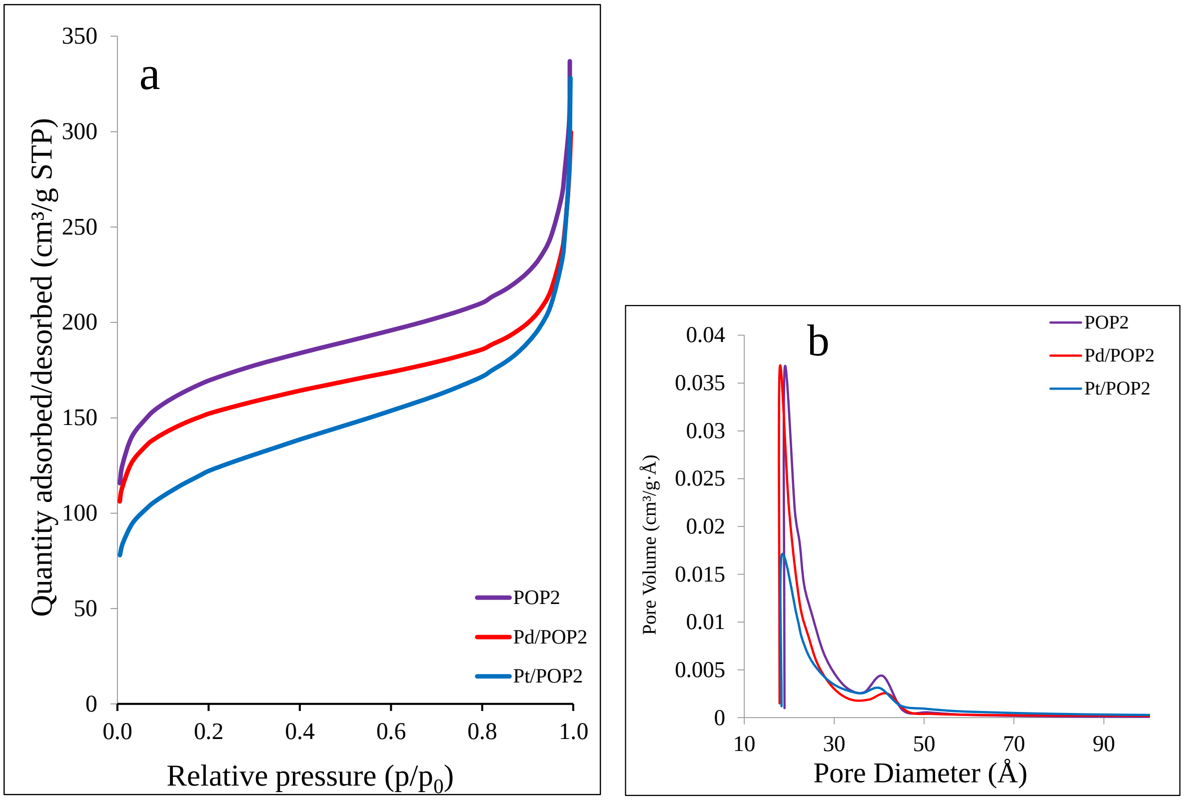

Figure 1. POP-based materials:(a) Nitrogen adsorption isotherms at -196 °C recorded on POP2 (purple), Pd/ POP2 (red), Pt/ POP2 (blue) (b) pore size distribution for the POP2 support and Pd/POP2 and Pt/POP2 catalysts

Table 1. Textural properties of the investigated materials (surface areas determined from Langmuir and Brunauer, Emmet, and Teller (BET), and pore size determined from Barrett, Joyner, and Halenda (BJH) and Horwath−Kawazoe methods.

Sample	BET surface area (m^2/g)	BJH pore size (Å)	Langmuir surface area (m^2g^{-1})	Horwath−Kawazoe pore size (Å)
POP1	377	21, 44	510	8.1
POP2	583	19, 41	787	8.2
POP3	271	20, 46	367	8.1
POP4	205	21,26, 44	292	8.3
0.5% Pd/POP1	339	21, 42	452	8.0
0.5% Pd/POP2	522	19, 40	704	8.0
0.5% Pd/POP3	241	20, 44	344	7.8
0.5% Pd/POP4	321	20, 43	411	8.0
0.5% Pt/ POP2	428	20, 41	587	8.1

Figure 2 depict the XRD patterns for the POP-based materials. They confirm the amorphous nature of the organic polymers (Figure 2a). The absence of reflection lines of copper species (POP1 support) and of palladium at 2θ 41° (POP2-POP4 supports) indicates that the small loadings of the remnant Sonogashira catalyst exist only in a highly dispersed state.[18] After the deposition-precipitation of the noble metals (Figure 2b,c), the recorded patterns shown that Pt is deposited in a high dispersion (no line, even after the reduction, Figure 2b), while Pd agglomerated after the reduction in hydrogen (line at 2θ 41°, Figure 2c).

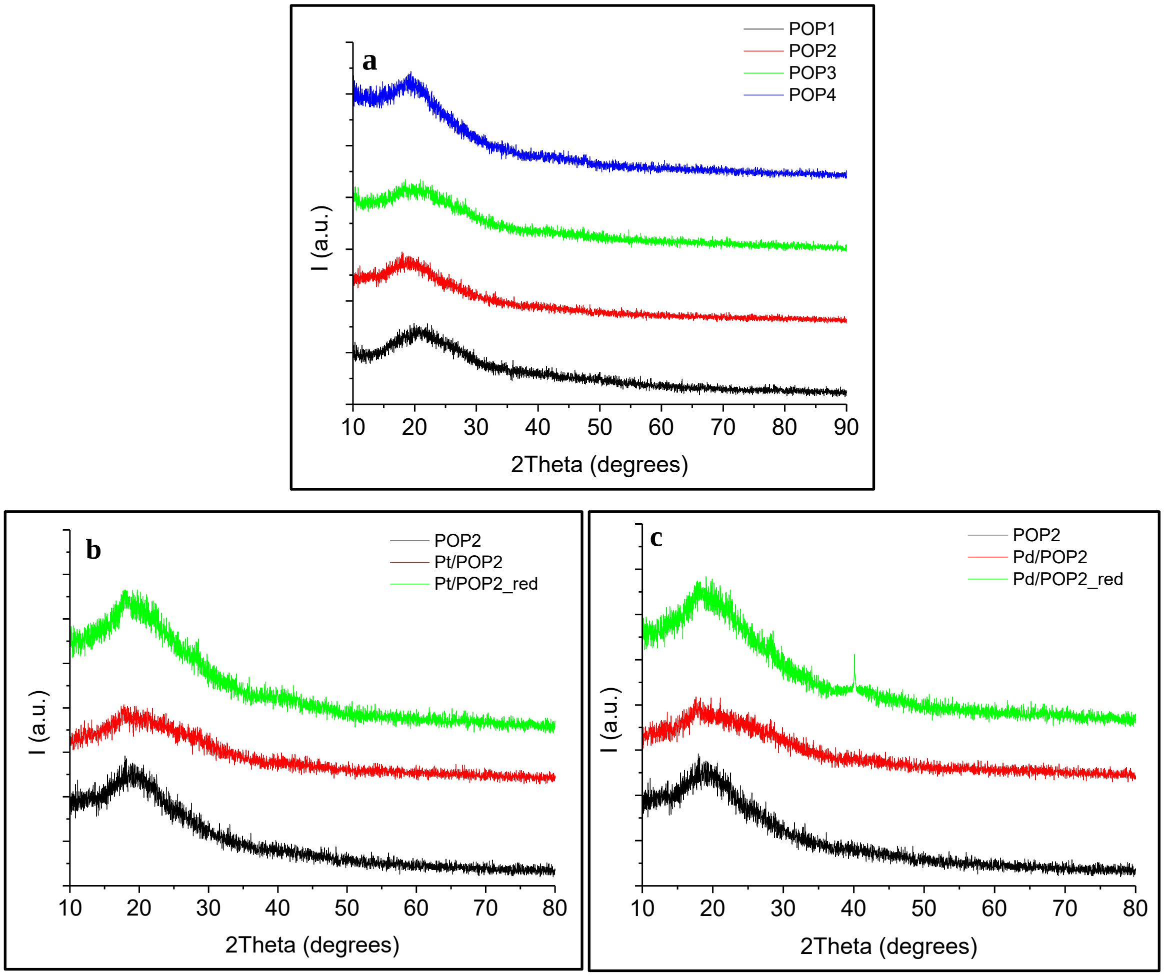

Figure 2. X-Ray Diffraction patterns for a) POP1-4 materials, b) POP2, un-reduced and H_2-reduced Pt/POP2 and c) POP2, un-reduced and H_2-reduced Pd/POP2

Figure 3 present XP spectra of the POP2 support and the investigated catalysts. For all the POP2-POP4 polymers, the XP spectra of the Pd 3d level present the typical Pd $3d_{5/2}$ and Pd $3d_{5/2}$ doublets confirming the presence of the remnant palladium in polymers (Figure 3a, Table 2). For the reduced POP2 (Figure 3a) the peaks located at binding energies of 336.2 and 341.2 eV are ascribed to zero-valent palladium,[40] while those at 337.7 and 342.6 eV to Pd^{2+} from the palladium complex catalyst used in the synthesis of POPs.[40,41] By calculating the integration areas of these two doublets, it can be estimated that, even after reduction, the incarcerated Pd^{2+} is the major phase in these polymers (approx. 88%).

Further deposition and reduction of palladium led to an increase in the intensity of the reduced Pd^0 species (Figure 3d). The doublets at 338.3 and 343.7 eV correspond to unreduced Pd^{2+}.[42] However, the Pd^{2+} species are still dominant (65%) after the reduction in hydrogen at 200 °C. An increase of the XPS Pd/C atomic ratio for the Pd/POP2 catalyst (Table 2) confirms the decrease of the dispersion by the deposition/precipitation method and is in line with the XRD results.

XPS also provided information about the state of the carbon in the POPs. The deconvolution of the C1s spectra for POP2 and Pd/POP2 samples (Figure 3 (b, e)) led to three components located at 284.6, 285.6 and 286.6 eV, respectively, that correspond to sp^2 and sp^3 C and C bonded to oxygen (C-O) species.[43] Further deposition of Pd on POP2, led to a more complex C spectrum evidencing the presence of C=O and COOH groups (287.6, 288.7 eV)[36] that well correlated to the concentration of the Pd^{2+} species.

The deconvolution of O1s spectra of POP2 and Pd/POP2 also point to the presence of the Pd^{2+} species (Figure 3 (c, f)). A peak with binding energy 533.2 eV was observed and is ascribed to Pd-O. The other two components in these spectra at 531.8 and 534.6 eV and were attributed to the oxygen bonded to aromatic structures (O-C-Ph, CH_3-O-Ph).[44]

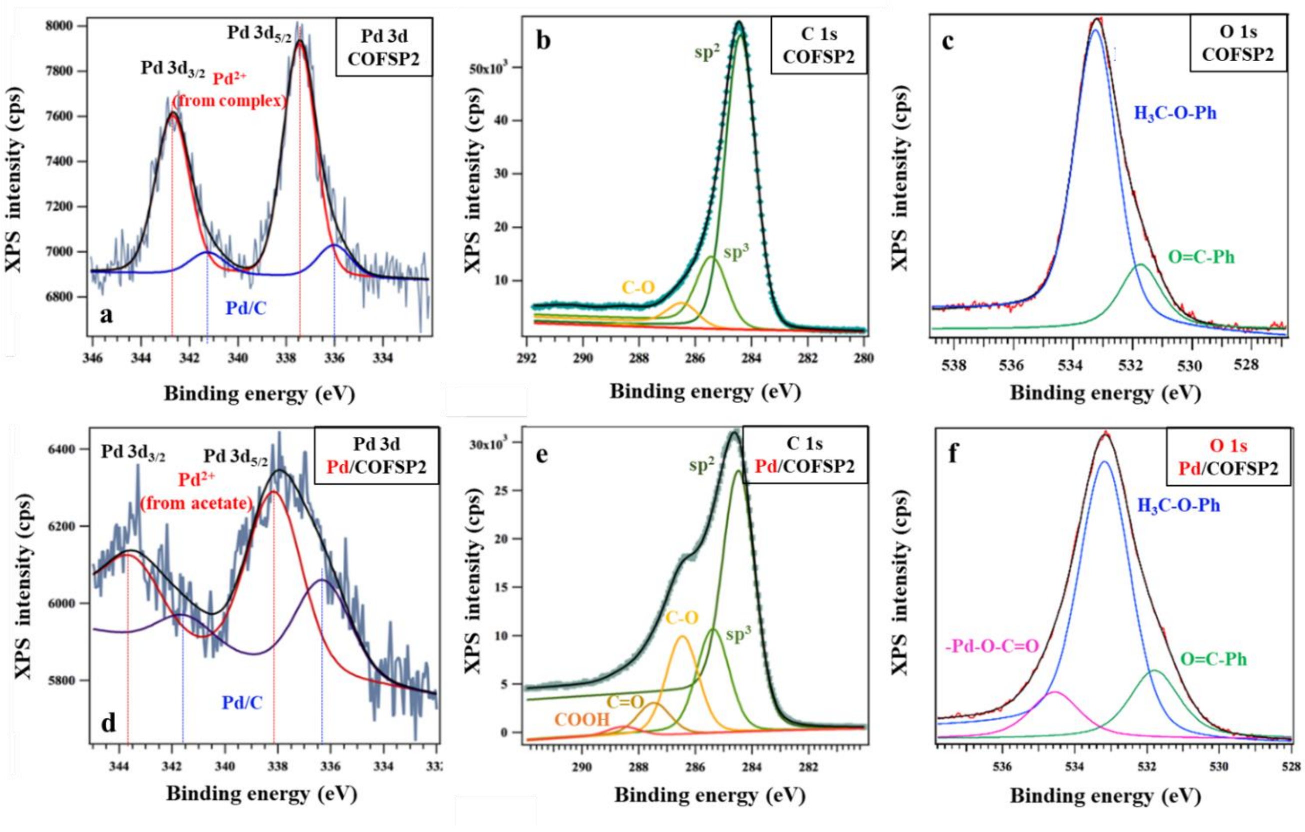

Figure 3. XP spectra of the Pd3d, C1s and O1s levels for the investigated materials

Table 2. XPS binding energies and Pd/C and Pd/(Pd+Pd^{2+}) ratios

Sample	Binding Energy (eV)		Species	XPS atomic ratio		Chemical Pd/C ratiox 10^2
	Pd 3d$_{5/2}$	Pd 3d$_{3/2}$		Pd/C	Pd(0)/(Pd(0)+Pd^{2+})x10^2	
POP2	336.2	341.2	Pd^0	5 x 10^{-3}	12	0.4
	337.7	342.5	Pd^{2+} from complex			
Pd/POP2	336.4	341.7	Pd^0	2 x 10^{-2}	35	3.0
	338.3	343.7	Pd^{2+}			

TEM analysis provided more insights in the characterization of these catalysts. The deposition of the palladium changed the morphology of the POP catalyst. TEM investigation of the POP2 sample reveals a flake-like morphology with an amorphous structure (Figure 4a), while the deposition of palladium (see Pd/POP2 sample) changed the morphology into a ball-like morphology (Figure 4b). It contains Pd nanoparticles with a diameter typically in the range of about 50 – 150 nm (Figure 4c,d). In the HAADF-STEM images, Pd is clearly visible as bright patches due to atomic number contrast (Z contrast; $Z_{Pd} = 46$)[45] This interpretation has been confirmed by EDXS point analysis (Figure 4d).

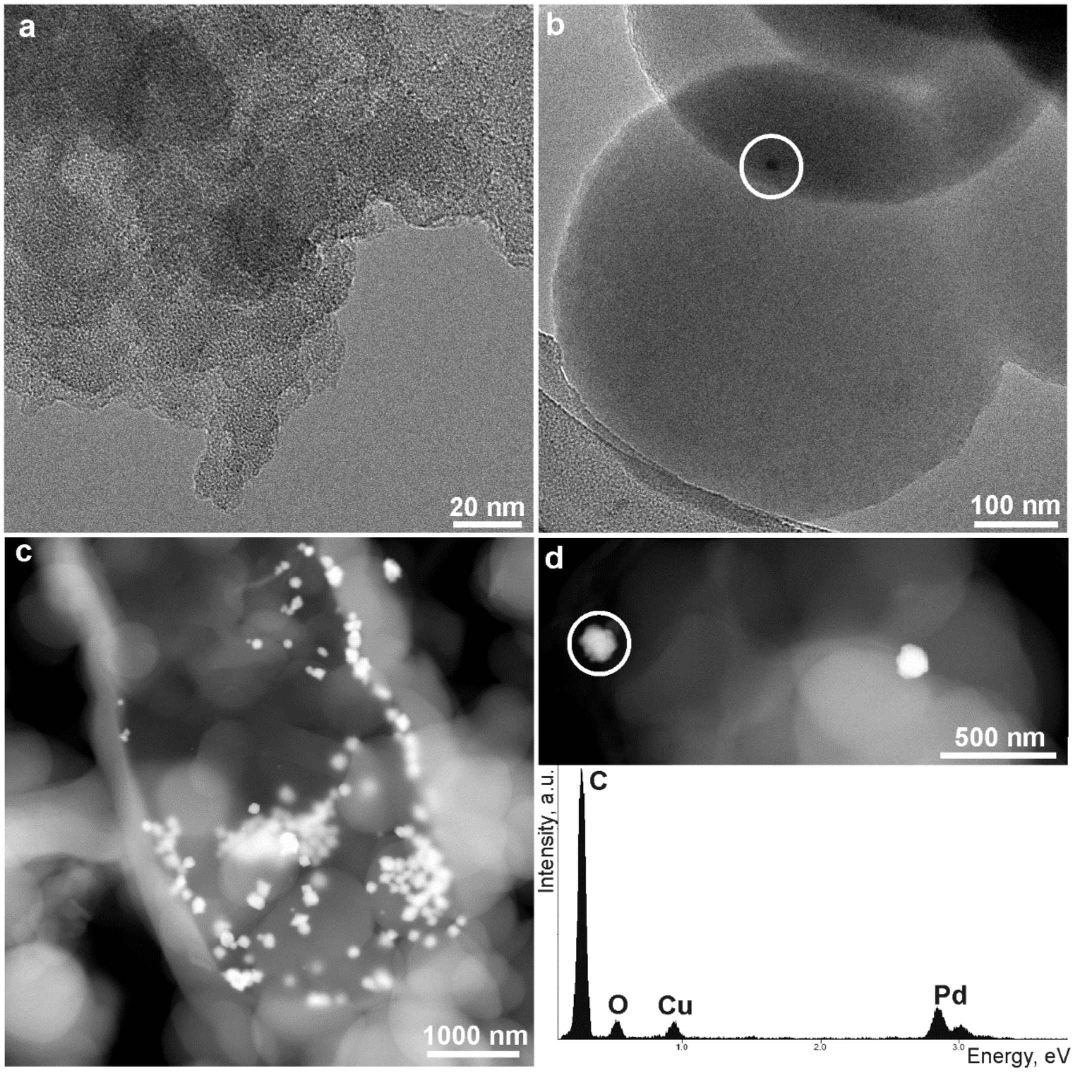

Figure 4. TEM images of a) the POP2 support and b) Pd/POP2 catalyst. In b), a Pd particle is encircled. c), d) HAADF-STEM images of Pd/POP2. c) shows an area with many 50 – 150 nm Pd nanoparticles. The EDX spectrum of the encircled particle in d) confirms the presence of Pd there. The Cu peak results from the supporting Cu TEM grid.

In the Pt/POP2 sample, the original morphology of POP2 is well preserved as recognized in the TEM image (Figure 5a). HAADF-STEM imaging (Figure 5b) reveals the homogeneous distribution of small Pt clusters that appear as bright dots (Z contrast). However, although highly dispersed, the deposition of Pt caused a more advanced decrease of the surface area and the pore size compared to Pd (Table 1). HAADF-STEM of the pure POP2 is not presented as it does not provide any new information.

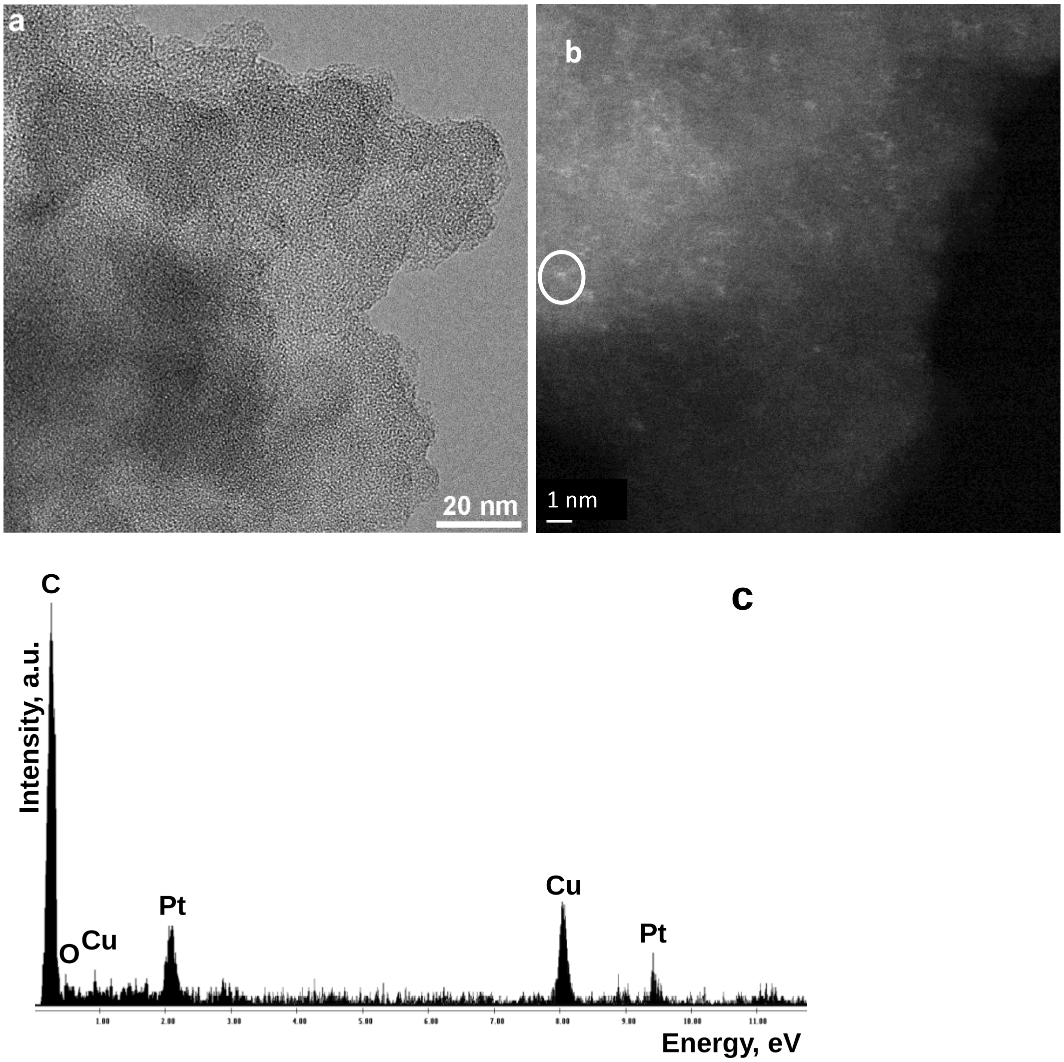

Figure 5. TEM a) and HAADF-STEM image b) of Pt/POP2. The EDX spectrum confirms the presence of Pt there. The Cu peak results from the supporting Cu TEM grid.

Catalytic activity

Hydrogenation of 4-nitrostyrene

10.1002/cctc.201801247

Catalytic tests with the synthesized POP1-4 polymers carried out in the hydrogenation of 4-NS (Scheme 3) show different activity and a full selectivity to 4-EN. Except for POP1, synthesised following a copper-based catalytic process, all other POPs are more active than a previously reported-adamantane based POP[16] (Table 3). These results are the consequence of the presence of residual Pd from the POP synthesis, well incarcerated in the polymer network and able to interact with 4-NS.[18]

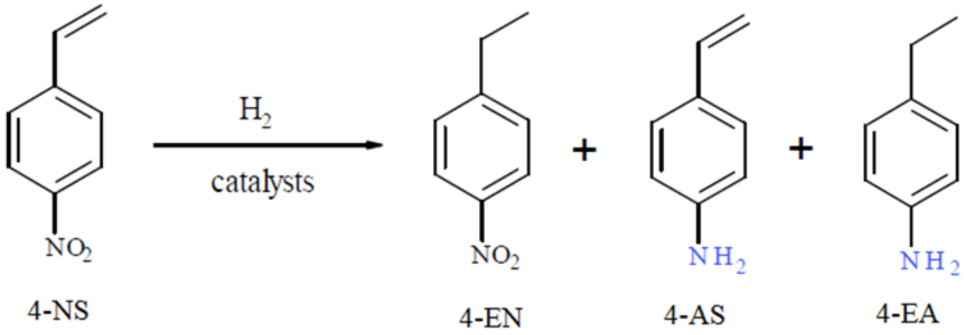

Scheme 3. Potential products of the hydrogenation of 4-NS

For POP2 the conversion increases from 8.3% after 1h to 80% after 6h, for POP3 from 1% to 43%, and for POP4 from 5.3% to 79%. Doing hot filtrated tests, the ICP-OES analysis of the reaction products indicated no palladium, thus eliminating the idea of any leaching of the active species.[46] Very important, all catalysts were recyclable in all the investigated reactions with the same performances (Figures SI6-10).

Table 3. Catalytic performance of POPs in the hydrogenation reaction of 4-NS

Entry	Catalyst	Time (h)	Conversion (%)	Selectivity (%) to		
				4-EN	4-AS	4-EA
1	POP1	1	0.1	100	0	0
2	POP2	1	8.3	100	0	0
3	POP3	1	1	100	0	0
4	POP4	1	5.3	100	0	0

5	POP1	6	0.1	100	0	0
6	POP2	6	80	100	0	0
7	POP3	6	45	100	0	0
8	POP4	6	79	100	0	0

Reaction conditions: 0.067 mmoles of 4-NS, 5 mL of heptane, 10 mg of catalyst, 25 atm H_2, temperature 90 °C)

The deposition of palladium onto POPs provided more active catalysts. They hydrogenate 4-NS at 1 atm hydrogen over 1 h with total or almost total conversions (Table 4). The comparison with a Pd/C show comparable activities but different selectivities. Pd/POP catalysts orientate this reaction mainly to 4-EN, while Pd/C in an almost equal selectivity to 4-EN and 4-EA. Pd/POPs also produced traces of 4-AS. Again, doing hot filtrated tests, the ICP-OES analysis of the reaction products indicated no palladium, thus eliminating the idea of any leaching of the active species.[46] Also important, all catalysts were recyclable with the same performances (Figures SI4-10).

Table 4. Catalytic performance of POPs in the hydrogenation reaction of 4-NS

Entry	Catalyst	Solvent	Time (h)	Conversion (%)	Selectivity (%) to		
					4-EN	4-AS	4-EA
1	Pd/POP1	Heptane	1	99	84	2	14
2	Pd/POP2	Heptane	1	100	86	5	9
4	Pd/POP3	Heptane	1	97	81	3	16
5	Pd/POP4	Heptane	1	99	82	3	15
6	Pd/C	Heptane	1	95	56	0	44
7	Pd/C	Ethanol	1	99	57	0	53

Reaction conditions: 0.067 mmoles of 4-NS, 5 mL of heptane, 10 mg of catalyst, 1 atm H_2, temperature 90 °C)

In spite of the small textural differences among these supports and differently to the carbon support the catalytic tests carried out in the hydrogenation of 4-NS shown no real effect on the palladium for the investigated hydrogenation reactions. Based on this, further catalytic tests used as reference catalyst the Pd/POP2 one.

Hydrogenation of 4-bromobenzophenone

Hydrogenation of 4-bromobenzophenone onto the same POPs provided further arguments in favour of the absence of leaching (Scheme 4, Table 5). First step corresponds to the hydrodehalogenation of the aromatic ring followed by the hydrogenation of the ketone. The remnant Pd in POPs can also catalyse the hydrodehalogenation of 4-BBP to benzophenone (**BP**). The conversion varied in the order POP4 > POP2 > POP3 ~ POP1 (Table 4). Among these, POP2, although in a small extent, was able to further hydrogenate the BP to diphenylmethanol (**DPM**) (selectivity of 7%).

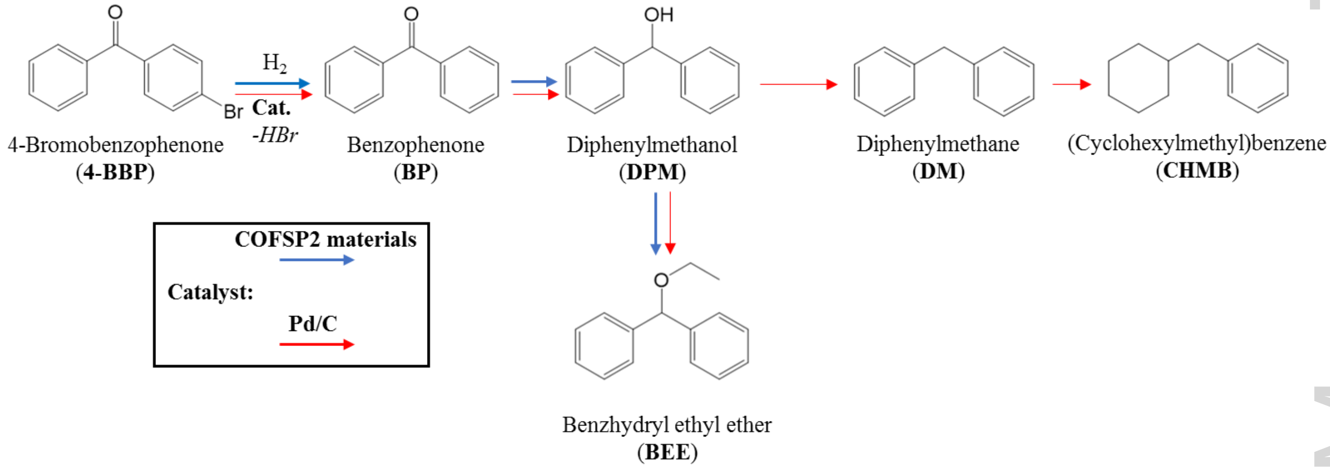

Scheme 4. Reaction scheme of the hydrogenation of 4-BBP

Table 5. Catalytic performance of POPs in the hydrogenation of 4-BBP

Entry	Catalyst	Time (h)	Conversion (%)	Selectivity (%) to	
				BP	DPM
1	POP1	6	0.6	100	0
2	POP2	6	18	93	7
3	POP3	6	15	100	0
4	POP4	6	60	100	0

Reaction conditions: 0.067 mmoles of 4-BBP, 5 mL of ethanol, 10 mg of catalyst, 25 atm H_2, temperature 80°C

Catalysts that are based on POPs supports behave different in this reaction than conventional catalysts do. Table 6 compiles comparative results for Pd/POP2 and carbon-based catalysts.

While the conversions are very similar, the use of the carbon as support provides a completely different selectivity. Pd/POP2 affords the selective hydrodehalogenation to BP with traces of BEE while Pd/C produces a further hydrolgenoysis of the C-O group to diphenylmethane (**DM**). Pd/C follows a more complex dehalogenation/hydrogenation/etherification pathway (Scheme 7). Using Pd/C, hydrogenation of the aromatic ring has also been observed, leading to (cyclohexylmethyl)benzene (**CHMB**) in small yields (Table 5). Operation at higher temperatures affords an advanced hydrodehalogenation to **BP** and hydrogenation/etherification of the produced OH groups to BEE in the detriment of **DM**.

Table 6. Catalytic results for 0.5 wt.% Pd catalysts for the hydrogenation of 4-BBP.

Entry	Catalyst	Temperature (°C)	Time (h)	Conversion (%)	Selectivity (%) to				
					BP	DPM	BEE	DM	CHMB
1	Pd/POP2	90	6	100	99.8	-	0.2	-	-
2	Pd/C	90	6	99	1.4	-	0.1	95	3.5
3	Pd/POP2	140	6	100	99.8	-	0.2	-	-
4	Pd/C	140	6	100	21.6	0.2	10.5	67	0.7

Reaction conditions: 0.067 mmoles of 4-BBP, 5 mL of ethanol, 10 mg of catalyst, 25 atm H_2

Table 6 provides additional evidence on the effect of temperature on the selective hydrogenation of 4-BBP over the investigated catalysts. The remnant Pd in POPs allows high conversion only at high temperatures. However, even in these conditions the reaction stops after hydrodehalogenation. With Pd- and Pt/POP catalysts, the conversion of the substrate is high, even at lower temperatures (i.e. 40 °C) with a very good selectivity in BP. Further increase of the reaction time to 24 h generates hydrogenation of a small amount of the dehalogenated ketone as evidenced by the formation of a very small quantity of BEE (almost 1%, Table 7). Hot filtration confirmed again the absence of leaching. No differences were observed between Pd and Pt.

The formation of benzhydryl ethyl ether (BEE) even in the small concentrations (Table 6) requires the presence of some catalytic acid sites. In these experiments, the acid source is only represented by the HBr released during the dehalogenation of the substrate. Its presence was well evidenced and quantified in the mixture collected after the reaction by the precipitation of AgBr with $AgNO_3$.

Table 7. Performances of the investigated catalysts for the hydrogenation of 4-BBP at different temperatures

Entry	Catalyst	Temperature (°C)	Time (h)	Conversion (%)	Selectivity (%) to		
					BP	DPM	BEE
1	POP2	90	6	20	100.00	-	-
2		140	6	60	100.00	-	-
3		180	6	100	99.70	-	0.3
4	Pd/POP2	40	6	92	99.80	-	0.2
5		60	6	100	99.80	-	0.2
6		90	6	100	99.80	-	0.2
7		140	6	100	99.80	-	0.2
8		180	6	100	99.70	-	0.3
9		180	24	100	98.90	-	1.1
10	Pt/POP2	90	6	100	99.70	-	0.3
11		140	6	100	99.79	0.01	0.2
12		180	6	100	99.68	0.02	0.3
13		180	24	100	99.08	0.02	0.9

Reaction conditions: 0.067 mmoles of 4-BBP, 5 mL of ethanol, 10 mg of catalyst, 25 atm H_2

The influence of the reaction time is presented for the hydrogenation of 4-BBP in the presence of the Pd/POP2 catalyst (90 °C, ethanol, 25 atm H_2) (Figure SI4). The deposition of the noble metals onto the POPs affords a fast reaction. For 0.5 wt% Pd, the conversion reached 16% with a

99% selectivity towards BP after 10 min (Figure SI4) and increases up to 95% after 2.5 h, and 99.8 % after 3 h.

Hydrogenation of acetophenone

The hydrogenation of acetophenone (ACP) on the investigated catalysts brings additional information about their catalytic behaviour. This reaction may lead to the corresponding phenyl alcohol as key intermediate for the production of fine chemicals, drugs and perfume industries.[47] Obviously it is achieved via homogeneous catalysis,[48] with the cost of the products separation and the recovery and reuse of the catalysts. For this reason, heterogeneous catalysts are highly demanded and there are already studies concerning the selective hydrogenation of ACP using catalysts containing noble metals (Pt, Pd, Rh, or Ru).[49] However, even in this case, the selective hydrogenation of ACP to 1-phenylethanol (1-PE) is not trivial, because different side reactions may take place, including the hydrogenation of the phenyl ring.

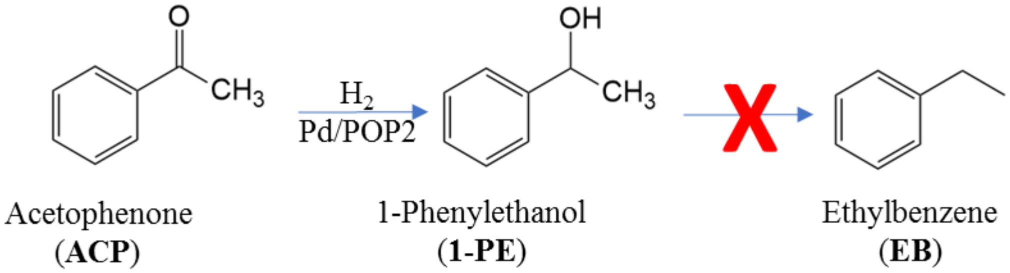

Scheme 5. Potential products of the hydrogenation of ACP

POP1-4 polymers exhibited no activity in the selective hydrogenation of ACP even after longer reaction times meaning that the remnant highly dispersed Pd catalyst is not capable of performance in such a reaction. However, the addition of 0.5 wt% Pd induced the required catalytic activity and the hydrogenation of ACP occurred with a selectivity of 100 % towards the desired 1-PE (Scheme 5).

Figure SI5 shows the evolution of the catalytic activity of Pd/POP2 as function of reaction time. After 1h, Pd/POP2 converts 8wt% of the substrate, 87wt% after 6h and 95wt% after 24h reaction time. A complete conversion was reached only after 30 h. Irrespective of the reaction time, the selectivity was preserved at 100% to 1-PE, and the catalyst was recyclable with the same performances.

Another important feature of these catalysts, in line to the literature, is that Pd supported catalysts induce the hydrogenolysis of C-OH providing ethylbenzene as a final product (Scheme 5).[50] However, this is not the case of the present catalysts which preserved the total selectivity towards 1-PE.

Hydrogenation of 7-nitro-1-tetralone

Catalytic tests for the selective hydrogenation of 7-nitro-1-tetralone (7N-1T) using POP2 and Pd/POP2 catalysts (Scheme 6) led to a mixture of 7-amino-α-tetralone (7A-αT), 7-nitro-1,2,3,4-tetrahydronaphthalene-1-ol (7N-THN) and 7-amino-1,2,3,4-tetrahydronaphthalene-1-ol (7A-THN). The results and the reaction conditions are summarized in Table 8.

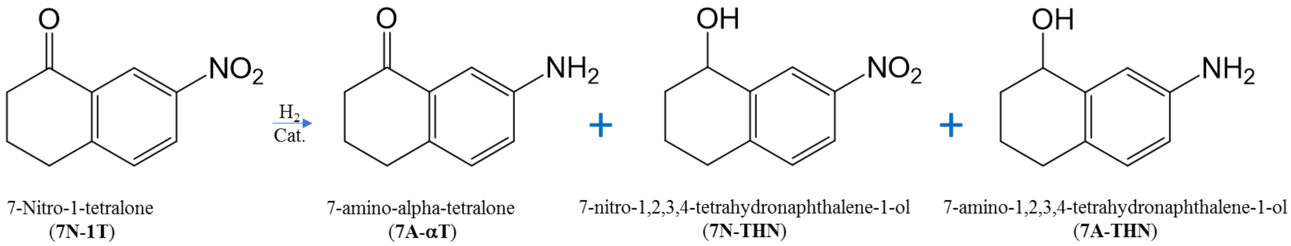

Scheme 6. Potential products of the hydrogenation of 7N-1T

The porous organic polymer is very active at relative low temperature (90 ˚C), where after 6 h reaction time the conversion was total with a selectivity of 80% to 7A-αT. The increase of the reaction temperature up to 140 ˚C practically had no catalytic consequences. However, the addition of 0.5 wt% Pd (Pd/POP2) changed the selectivity. At 90 ˚C, the selectivity to 7A-THN increased at 35% on the cost of the decrease of the selectivity to 7A-αT, while at 140 ˚C it produces a further decrease in the selectivity to 7A-αT forming 7N-THN (Scheme 6). This behaviour is indicative for a structural sensitive reaction requiring larger Pd nanoparticles.

By increasing the reaction time from 6 to 24 h, in the presence of Pd/POP2, the selectivity towards 7A-αT suffered a drastic decrease. After 24 h it decreased to 36% compared to 63% after 6h. Since the yield in the nitro alcohol remained unchanged, it is likely that the hydrogenation of 7N-1T occurs mainly via the hydrogenation of the nitro-group to 7A-αT, which further it is hydrogenated to the aminoalcohol.

Table 8. Hydrogenation of 7-nitro-1-tetralone onto the investigated catalysts

Entry	Catalyst	t (°C)	Time (h)	Conversion (%)	Selectivity (%) to		
					7A-αT	**7N-THN**	**7A-THN**
1	POP2	90	6	**100**	80	4	16
2		140	6	**100**	78	3	19
3	Pd/ POP2	90	6	**100**	63	2	35
4		140	6	**100**	58	8	34
5		90	24	**100**	36	5	59

Reaction conditions: 0.067 mmoles of 7N-1T, 5 mL of ethanol, 10 mg of catalyst, 25 atm H_2

Hydrogenation of 1,2-Naphtoquinone

Table 9 compiles results collected from the hydrogenation of 1,2-naphthoquinone (1,2NQ) (Scheme 7) in the presence of Pd/POP2 and Pt/POP2. The main reaction products were 1-hydroxy-1H-naphthalen-2-one (1H1HN) and 1,2-dyhydroxynaphthalene-1,2-diol (1,2DHN). Hydrogenation of 1,2NQ occurred only at high temperature (see Table 8), and with relative low conversion compared to the other substrates. However, the 0.5wt% Pt/POP2 was more active (59 versus 22% conversion) but less selective toward 1,2DHN (8 versus 72%) compared to the corresponding Pd/POP2. Pd afforded a more advanced hydrogenation of both carbonyl groups.

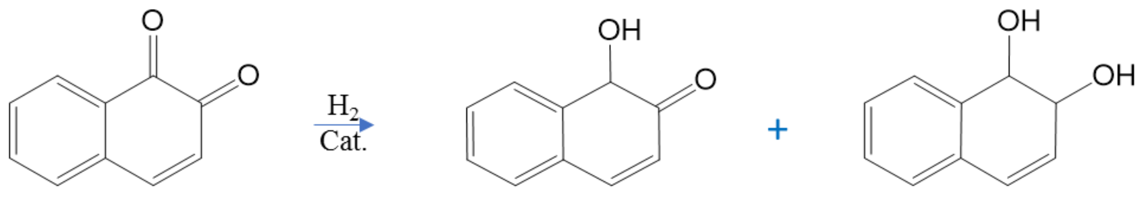

1,2-Naphthoquinone
(1,2NQ)

1-Hydroxy-1H-naphthalen-2-one
(1H1HN)

1,2-Dihydroxynaphthalene-1,2-diol
(1,2DHN)

Scheme 7. Potential products of the hydrogenation of 1,2NQ

Table 9. Hydrogenation of 1,2-naphthoquinone onto the investigated catalysts

Entry	Catalyst	t (°C)	Time (h)	Conversion (%)	Selectivity (%) to	
					1H1HN	1,2DHN
1	Pd/ POP2	140	6	**-**	-	-
2		180	6	**22**	28	72
3	Pt/ POP2	140	6	**-**	-	-
4		180	6	**59**	92	8

Reaction conditions: 0.067 mmoles of 1,2NQ, 5 mL of ethanol, 10 mg of catalyst, 25 atm H_2

The performance of the catalysts in this reaction was strongly influenced by the solvent properties, namely, by its polarity (dielectric constant, ε). Thus, the hydrogenation of 4-BBPh in ethanol (ε= 24.55 at 20 °C[44]) afforded higher conversions than in n-heptane (**(**ε=1.92 at 20 °C[51]) (Table 10). The superior activity of the Pd catalysts in ethanol compared to heptane is in very good accordance with literature.[52] Changing the metal has no essential influence in this reaction.

Table 10. Performances of the investigated catalysts for the hydrogenation of 4-BBP using different solvents

Entry	Catalyst	Solvent	Time (h)	Conversion (%)	S (%)		
					BP	DPM	BEE
1	POP2_red	Ethanol	6	20	100.0	-	-
2		Heptane	6	0.4	100.0	-	-
3	Pd/POP2_red	Ethanol	6	100	99.8	-	0.2
4		Heptane	6	10	100.0	-	-

5	Pt/POP2_red	Ethanol	6	100	99.7	-	0.3
6		Heptane	6	16	100	-	-

Reaction conditions: 0.067 mmoles of 4-BBP, 5 mL of solvent, 10 mg of catalyst, 25 atm H_2, temperature 90 °C

Catalysts stability

The experiments considering the Sheldon's hot filtration test. [52] confirmed the absence of any leaching. Besides this, TEM characterizations did not show any rearrangement/agglomeration of the metal nanoparticles or morphology change after the reaction.

Conclusions

Spirobifluorene-based porous organic polymer frameworks synthesized following two different protocols (the acetylenic coupling reaction conditions and the Sonogashira cross-coupling reaction) behaved differently in the investigated hydrogenation reactions. POP1 prepared via a copper-catalysis protocol was completely inactive, while POP2-4 exhibited different activities in accordance to the accessibility of the substrates to the residual Pd. The deposition of Pd led to active and stable catalysts in the investigated reactions in which the differences in the POP properties exhibited either very small or no effect. They were easily separated by filtration and after re-dispersion afforded the same performances for 10 successive cycles. The performances of these catalysts in the hydrogenation of 4-nitrostyrene, 4-bromobenzophenone, acetophenone, 7-nitro-1-tetralone and 1,2-naphtoquinone confirmed their efficiency.

However, the role of these supports show specific properties. This has been demonstrated by the behaviour of the different 0.5wt% Pd-POP catalysts in a very good correlation to their structural characteristics, but also by the comparison with a Pd/C catalyst with the same loading of palladium. The catalytic experiments revealed the role of the active metal. Platinum interacts differently with the support affording sub-nanometric particles and, in accordance, a different catalytic behaviour reflected merely by differences in the selectivity of the hydrogenation of 1,2-naphthoquinone.

10.1002/cctc.201801247

Experimental Section

Synthesis of POPs

The spirobifluorene-based covalent organic frameworks were obtained quantitatively either from the tetraethynyl derivative **6** submitted to the acetylenic coupling reaction conditions (Scheme 8), or via the Sonogashira cross-coupling reactions of tetraiodo derivative **4** with 1,4-diethynylbenzene **7** or 4,4'-diethynyl-biphenyl **8** (Scheme 9).

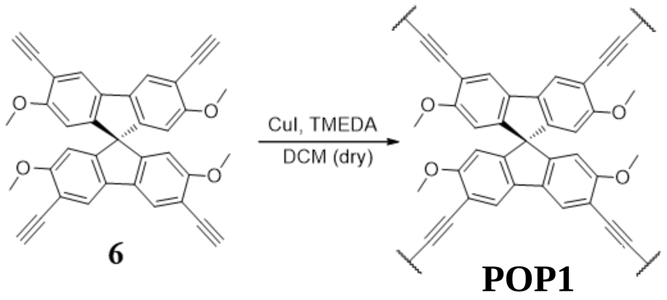

Scheme 8

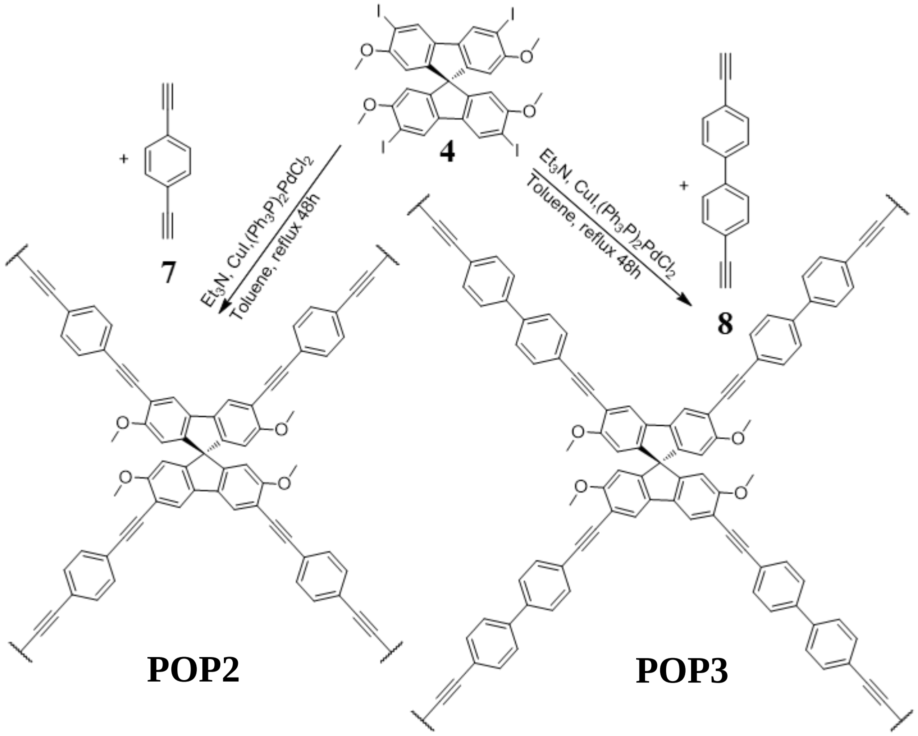

Scheme 9

All attempts to obtain POPs starting from the tetraiodurated derivative **2** *via* the acetylenic coupling and the Sonogashira cross-coupling reactions with **7** and **8** failed due to the geometry constraints induced by the macromolecules. However, the Sonogashira cross-coupling protocol was successful by reacting **2** with *meta*-diethynylbenzene **9** (Scheme 10) probably due to the geometry correction and to the tetrahedral structure of POP4.

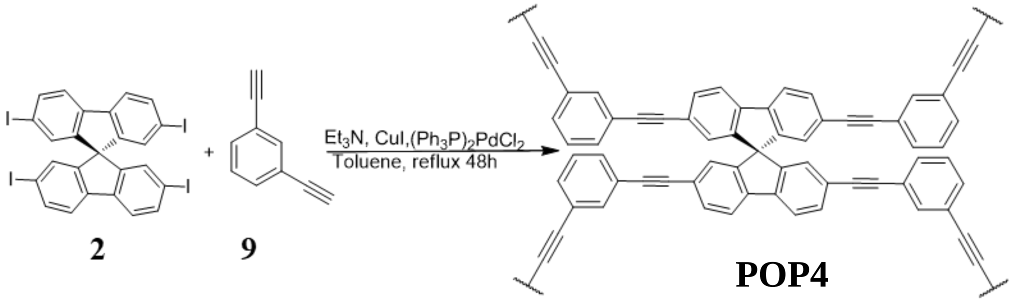

Scheme 10

Procedure for the access to POP1

The mixture formed of terminal tetraalkyne **6** (2,2',7,7'-Tetramethoxy-3,3',6,6'-tetraethynyl-9,9'-spirobifluorene), (0.1 g, 0.17 mmoles), tetramethylethylenediamine (0.44 g, 3.8 mmoles), and CuI (0.21 g, 1.1 mmoles) in dry DCM (20 mL) under an aerobe atmosphere (supplied by bubbling air into the reaction mixture) was stirred at room temperature for 12 h. At the end the solid was collected by filtration, washed with dichloromethane, methanol, water and dried to quantitatively yield ***POP1.***

General procedure for the access to POP2-POP4

2,2',7,7'-Tetramethoxy-3,3',6,6'-tetraiodo-9,9'-spirobifluorene **4** (0.1 g, 0.1 mmoles) was dissolved in dry toluene (15 mL) and Et_3N (1 mL), then the solution was flushed with argon for 20 min. The diethynyl derivative [1,4-diethynylbenzene **7** (0.06 g, 0.44 mmoles) for POP2; 4,4′-diethynylbiphenyl **8** (0.09 g, 0.44 mmoles) for POP3 or 1,3-diethynylbenzene **9** (0.1 g, 0.1 mmoles) for POP4], $PdCl_2(PPh_3)_2$ (11 mg, 0.016 mmoles) and CuI (3 mg, 0.016 mmoles) were added under argon atmosphere, and the reaction mixture was stirred under reflux (110 °C) for 48 h. At the end, after cooling the reaction mixture at room temperature, the solid was collected by filtration, washed with dichloromethane, methanol and water, and dried to give quantitatively POP2-4 as a pale brown powder.

Synthesis of Pd/POP1-4, Pt/POP2 and Pd/C catalysts via the deposition-precipitation method

Pd/POP1-4 and Pt/POP2 catalysts (with 0.5 wt. % noble metal) were prepared starting from a 0.3 mM precursor solution [$Pd(CH_3COO)_2$ or H_2PtCl_6, respectively] in 30 mL of methanol. The deposition-precipitation of the metal was achieved with an aqueous solution of ammonia (25wt%) at pH=9 in the presence of the corresponding amount of the support (POP). The stirring was continued for another 2h, and then the supported solid was washed with distilled water, dried at 80 °C for 2h under vacuum and at 80 °C overnight. Finally, Pd/POP1-4 and Pt/POP2 were reduced under a hydrogen flow (30 mL/min) at 200 °C for 3h. The synthesis of the Pd/C based catalyst was described elsewhere [18].

Textural and structural characterization of the catalysts

Thermogravimetric (TG) and differential thermal analysis (DTA) were performed with a Shimadzu DTG- 60 instrument under a dry nitrogen flow (50 mL/min, from Linde, purity 99.996%) in the temperature range 25–800 ºC with a heating-up rate of 5 ºC/min. Textural characterization of the POPs and catalysts was carried out by measuring the adsorption−desorption isotherms of nitrogen at -196 °C on a fully computerized Micromeritics ASAP 2020 instrument, using the BET and Langmuir formalisms. Before the analysis, the powders were degassed at 150 °C till a pressure of 10^{-6} atm. Powder X-ray diffraction (XRD) patterns were recorded on a Shimadzu XRD-7000 diffractometer using the Cu Kα radiation (λ = 1.5418 Å, 40 kV, 40 mA) at a scanning rate of 0.10-2θ/min in the 2θ range 10-80°. For TEM and EDX, the samples were dispersed in ethanol and some droplets of the suspension were deposited on a lacey carbon foil supported on a Cu grid or supported on an aluminium stub, respectively.

TEM was performed on a Tecnai F30 (FEI, field emission gun (FEG), SuperTwin lens (point resolution ca. 0.2 nm), operated at 300 kV. EDX investigations were performed with an LEO 1530 Gemini (Zeiss, operated at 1 kV) or with a Quanta 200 (FEI, operated at 5 kV) equipped with an EDX spectrometer (EDAX). X-ray photoelectron spectroscopy (XPS) measurements were carried out on a SPECS surface-science cluster, including an XPS spectrometer equipped with a monochromatic Al Kα1 X-ray source (photon energy 1486.74 eV) and operating under ultrahigh vacuum at $1.3\cdot10^{-13}$ atm. The photoelectrons were collected by a 150 mm radius Phoibos electron analyzer with a pass energy of 30 eV, resulting in a full width at half maximum (FWHM) of the Au 4f7/2 core levels of 1.15 eV55. The binding energies were corrected for the surface-charging effects during the measurements by using the C1s core level (284.6 eV) of the adventitious carbon as an internal reference. The content of palladium was determined by ICP-OES (Agilent Technologies, 700 Series) after calibrating the instrument with standard solutions.

Catalytic tests

The catalytic tests were carried out in the hydrogenation of a series of unsaturated compounds (4-nitrostyrene (4-NS), (acetophenone (ACP), 4-bromobenzophenone (4-BBP), 1,2-naphtoquinone (1,2-NQ) and 7-nitro-1-tetralone (7N-1T)) of Sigma-Aldrich purity. All the reactions were carried out in a magnetically stirred 25 mL stainless steel autoclave. Typically, 10 mg of catalyst were added together with 0.067 mmoles of substrate and 5 mL of solvent. The autoclave was purged with H_2 for 3 times to remove the air and then pressurized with molecular hydrogen at 25 atm. The reactions were carried out at 40-180 ºC for different reaction times (from 0.16 to 24 h). After reaction, the catalyst and the liquid were separated by filtration and reaction products were analysed by gas chromatography using a GC 2014 Shimadzu apparatus equipped with a DB-5MS capillary column (0.20 mm x 50 m x 0.33 µm) and flame ionization detector (FID).

Leaching evaluation has been carried out using the Sheldon's hot filtration test. [52] After 4h the catalyst was filtered while maintaining the mixture at the reaction temperature. The filtrate was then stirred at the same temperature for an additional 4h. Quantitative analyses were carried out by GC (to evaluate the conversion) and ICP-OES (to evaluate the leached Pd or Pt). The recyclability of the catalysts has been checked in.

Acknowledgements

CNCS/CCCDI – UEFISCDI, project numbers PN-III-P2-2.1-PED-2016-0349

Conflict of interest

The authors declare no conflict of interest.

References

[1] M. Ito, T. Ikariya, *Chem. Commun.* **2007**, 5134-5142.

[2] a) C. Hedberg, in *Mod. Reduct. Methods*, Wiley-VCH Verlag GmbH & Co. KGaA, **2008**, pp. 107-134; b) M. Gopiraman, S. G. Babu, Z. Khatri, K. Wei, M. Endo, R. Karvembu, I. S. Kim, *Catal. Sci. Technol.* **2013**, *3*, 1485-1489.

[3] R. Montalvo-González, D. Chávez, G. Aguirre, M. Parra-Hake, R. Somanathan, *Synth. Commun.* **2009**, *39*, 2737-2746.

[4] a) G. C. Bond, *Chem. Soc. Rev.* **1991**, *20*, 441-475; b) U. K. Singh, M. A. Vannice, *Appl. Catal., A:Gen. A* **2001**, *213*, 1-24; c) P. Gallezot, D. Richard, *Catal. Rev.* **1998**, *40*, 81-126; d) A. Corma, P. Serna, P. Concepción, J. J. Calvino, *J. Am. Chem. Soc.* **2008**, *130*, 8748-8753; e) F. Neatu, A. Kraynov, V. I. Parvulescu, K. Kranjc, M. Kocevar, V. Ratovelomanana-Vidal, R. Richards, *Nanotechnology* **2008**, *19*, 225702.

[5] A. Corma, P. Serna, *Science* **2006**, *313*, 332-334.

[6] a) L. M. Rossi, F. P. Silva, L. L. R. Vono, P. K. Kiyohara, E. L. Duarte, R. Itri, R. Landers, G. Machado, *Green Chem.* **2007**, *9*, 379-385; b) F. A. Harraz, S. E. El-Hout, H. M. Killa, I. A. Ibrahim, *J. Catal.* **2012**, *286*, 184-192; c) D. Astruc, F. Lu, R. Aranzaes Jaime, *Angew. Chem., Int. Ed.* **2005**, *44*, 7852-7872.

[7] R. J. White, R. Luque, V. L. Budarin, J. H. Clark, D. J. Macquarrie, *Chem. Soc. Rev.* **2009**, *38*, 481-494.

[8] a) T. T. Upadhya, S. P. Katdare, D. P. Sabde, V. Ramaswamy, A. Sudalai, *Chem. Commun.* **1997**, 1119-1120; b) R. A. W. Johnstone, A. H. Wilby, I. D. Entwistle, *Chem. Rev.* **1985**, *85*, 129-170.

[9] a) R. Prins, *Chem. Rev.* **2012**, *112*, 2714-2738; b) W. Karim, C. Spreafico, A. Kleibert, J. Gobrecht, J. VandeVondele, Y. Ekinci, J. A. van Bokhoven, *Nature* **2017**, *541*, 68.

[10] a) M. Tian, X. Cui, M. Yuan, J. Yang, J. Ma, Z. Dong, *Green Chem.* **2017**, *19*, 1548-1554; b) X. Chen, L. Zhang, B. Zhang, X. Guo, X. Mu, *Sci. Rep.* **2016**, *6*, 28558; c) P. Serp, M. Corrias, P. Kalck, *Appl. Catal., A:Gen.* **2003**, *253*, 337-358; d) S. Navalon, A. Dhakshinamoorthy, M. Alvaro, H. Garcia, *Coord. Chem. Rev.* **2016**, *312*, 99-148.

[11] a) P. Kuhn, M. Antonietti, A. Thomas, *Angew. Chem. Int. Ed.* **2008**,*47*, 3450–3453; b) P. Kuhn, A.I. Forget, D. Su, A. Thomas, M. Antonietti, *J. Am. Chem. Soc.* **2008**, *130*, 13333–13337; c) P. Kuhn, A.I. Forget, J. Hartmann, A. Thomas, M. Antonietti, *Adv. Mater.* **2009,** *21*, 897–901; d) S. Ren, M.J. Bojdys, R. Dawson, A. Laybourn, Y.Z. Khimyak, D.J. Adams, A.I. Cooper. *Adv. Mater.* **2012**, *24*, 2357–2361; e) R. Palkovits, M. Antonietti, P. Kuhn, A. Thomas, F. Schuth, *Angew. Chem. Int. Ed.* **2009**, *48*, 6909–6912; f) M. Rose, *ChemCatChem* **2014**, *6*, 1166–1182; g) J. Roeser, K. Kailasam, A. Thomas, *ChemSusChem* **2012**, *5*, 1793–1799.

[12] a) N.B. McKeown, P.M. Budd, *Chem. Soc. Rev.* **2006**, *35*, 675-683; b) Z. Wang, G. Chem, K.L. Ding, *Chem. Rev.* **2009**, *109*. 322-359; c) A.I. Cooper, *Adv. Mater.* **2009**, *21*, 1291-1295.

[13] S.Y. Ding, J. Gao, Q. Wang, Y. Zhang, W. G. Song, C.Y. Su, W. Wang, *J. Am. Chem. Soc.* **2011**, *133*, 19816–19822.

[14] a) P. Kaur, J.T. Hupp, S.T. Nguyen, *ACS Catal.* **2011**, *1*, 819-835; b) Z. Xie, C. Wang, K. E. de Krafft, W. Lin, *J. Am. Chem. Soc.* **2011**, *133*, 2056-2059.

[15] a) H.-C. Ma, J.-L. Kan, G.-J. Chen, C.-X. Chen, Y.-B. Dong, *Chem. Mater.* **2017**, *29*, 6518−6524; b) G.-J. Chen, X.-B. Li, C.-C. Zhao, H.-C. Ma, J.-L. Kan, Y.-B. Xin, C.-X. Chen, Y.-B. Dong, *Inorg. Chem.* **2018**, *57*, 2678-2685.

[16] a) M. Shunmughanathan, P. Puthiaraj, K. Pitchumani, *ChemCatChem*, **2015**, *7*, 666-673; b) Y.-B. Zhou, C.-Y. Li, M. Lin, Y.-J. Ding, Z.-P. Zhan, *Adv. Synth. Catal.* **2015**, *357*, 2503 –2508; c) R.S.B. Goncalves, A.B.V. de Oliveira, H.C. Sindra, B.S. Archanjo, M.E. Mendoza, L.S.A. Carneiro, C.D. Buarque, P.M. Esteves, *ChemCatChem* **2016**, *8*, 743 – 750; d) Y.-B. Zhou, Y.-Q. Wang, L.-C. Ning, Z.-C. Ding, W.-L. Wang, C.-K. Ding, R.-H. Li, J.-J. Chen, X. Lu, Y.-J. Ding, Z.-P. Zhan, *J. Am. Chem. Soc.* **2017**, *139*, 3966-3969; e) Y. Monguchi, F. Wakayama, S. Ueda, R. Ito, H. Takada, H. Inoue, A. Nakamura, Y. Sawamaa, H. Sajiki, *RSC Adv.* **2017**, *7*, 1833; f)

Z.-C. Ding, C.-Y. Li, J.-J. Chen, J.-H. Zeng, H.-T. Tang, Y.-J. Ding, Z.-P. Zhan, *Adv. Synth. Catal.* **2017**, *359*, 2280 – 2287; g) L.-P. Jing, J.-S. Sun, F. Sun, P. Chen, G. Zhu, *Chem. Sci*. **2018**, *9*, 3523–3530.

[17] W.-H. Li, C.-Y. Li, Y. Li, H.-T. Tang, H.-S. Wang, Y.-M. Pan, Y.-J. Ding, *Chem. Commun.* **2018**, *54*, 8446—8449.

[18] M. M. Trandafir, L. Pop, N. D. Hadade, M. Florea, F. Neatu, C. M. Teodorescu, B. Duraki, J. A. van Bokhoven, I. Grosu, V. I. Parvulescu, H. Garcia, *Catal. Sci. Technol.* **2016**, *6*, 8344-8354.

[19] a) Q. Fang, S. Gu, J. Zheng, Z. Zhuang, S. Qiu, Y. Yan, *Angew. Chem., Int. Ed.* **2014**, *53*, 2878-2882; b) L. Li, H. Zhao, R. Wang, *ACS Catal.* **2015**, *5*, 948-955.

[20] S. M. J. Rogge, A. Bavykina, J. Hajek, H. Garcia, A. I. Olivos-Suarez, A. Sepulveda-Escribano, A. Vimont, G. Clet, P. Bazin, F. Kapteijn, M. Daturi, E. V. Ramos-Fernandez, F. X. Llabres i Xamena, V. Van Speybroeck, J. Gascon, *Chem. Soc. Rev.* **2017**, *46*, 3134-3184.

[21] W. Lu, D. Yuan, D. Zhao, C. I. Schilling, O. Plietzsch, T. Muller, S. Bräse, J. Guenther, J. Blümel, R. Krishna, Z. Li, H.-C. Zhou, *Chem. Mater.* **2010**, *22*, 5964-5972.

[22] a) J. Chun, S. Kang, N. Park, E. J. Park, X. Jin, K.-D. Kim, H. O. Seo, S. M. Lee, H. J. Kim, W. H. Kwon, Y.-K. Park, J. M. Kim, Y. D. Kim, S. U. Son, *J. Am. Chem. Soc.* **2014**, *136*, 6786-6789; b) S.-Y. Moon, H.-R. Mo, M.-K. Ahn, J.-S. Bae, E. Jeon, J.-W. Park, *J. Polym. Sci., Part A: Polym. Chem.* **2013**, *51*, 1758-1766; c) D. Beaudoin, T. Maris, J. D. Wuest, *Nat. Chem.* **2013**, *5*, 830-834.

[23] J. Dong, Y. Liu, Y. Cui, *Chem. Commun.* **2014**, *50*, 14949-14952.

[24] T. Muller, S. Brase, *RSC Adv.* **2014**, *4*, 6886-6907.

[25] H. Yu, C. Shen, M. Tian, J. Qu, Z. Wang, *Macromolecules* **2012**, *45*, 5140-5150.

[26] R. Dawson, A. I. Cooper, D. J. Adams, *Prog. Polym. Sci.* **2012**, *37*, 530-563.

[27] D. Yuan, W. Lu, D. Zhao, H.-C. Zhou, *Adv. Mater.* **2011**, *23*, 3723-3725.

[28] J. Schmidt, M. Werner, A. Thomas, *Macromolecules* **2009**, *42*, 4426-4429.

[29] R. T. Woodward, L. A. Stevens, R. Dawson, M. Vijayaraghavan, T. Hasell, I. P. Silverwood, A. V. Ewing, T. Ratvijitvech, J. D. Exley, S. Y. Chong, F. Blanc, D. J. Adams, S. G. Kazarian, C. E. Snape, T. C. Drage, A. I. Cooper, *J. Am. Chem. Soc.* **2014**, *136*, 9028-9035.

[30] a) Q. Chen, M. Luo, T. Wang, J.-X. Wang, D. Zhou, Y. Han, C.-S. Zhang, C.-G. Yan, B.-H. Han, *Macromolecules* **2011**, *44*, 5573-5577; b) K. V. Rao, S. Mohapatra, C. Kulkarni, T. K. Maji, S. J. George, *J. Mater. Chem.* **2011**, *21*, 12958-12963.

[31] a) J.-X. Jiang, F. Su, A. Trewin, C. D. Wood, H. Niu, J. T. A. Jones, Y. Z. Khimyak, A. I. Cooper, *J. Am. Chem. Soc.* **2008**, *130*, 7710-7720; b) R. Dawson, A. Laybourn, R. Clowes, Y. Z. Khimyak, D. J. Adams, A. I. Cooper, *Macromolecules* **2009**, *42*, 8809-8816.

[32] T. Ben, H. Ren, S. Ma, D. Cao, J. Lan, X. Jing, W. Wang, J. Xu, F. Deng, J. M. Simmons, S. Qiu, G. Zhu, *Angew. Chem., Int. Ed.* **2009**, *48*, 9457-9460.

[33] a) E. L. Spitler, M. R. Giovino, S. L. White, W. R. Dichtel, *Chem. Sci.* **2011**, *2*, 1588-1593; b) A. L. Korich, P. M. Iovine, *Dalton Trans.* **2010**, *39*, 1423-1431; c) M. K. Smith, B. H. Northrop, *Chem. Mater.* **2014**, *26*, 3781-3795.

[34] a) G. Das, D. Balaji Shinde, S. Kandambeth, B. P. Biswal, R. Banerjee, *Chem. Commun.* **2014**, *50*, 12615-12618; b) Y.-B. Zhang, J. Su, H. Furukawa, Y. Yun, F. Gándara, A. Duong, X. Zou, O. M. Yaghi, *J. Am. Chem. Soc.* **2013**, *135*, 16336-16339; c) M. E. Belowich, J. F. Stoddart, *Chem. Soc. Rev.* **2012**, *41*, 2003-2024.

[35] X. Zhu, C. Tian, T. Jin, J. Wang, S. M. Mahurin, W. Mei, Y. Xiong, J. Hu, X. Feng, H. Liu, S. Dai, *Chem. Commun.* **2014**, *50*, 15055-15058.

[36] a) Y. Du, K. Mao, P. Kamakoti, P. Ravikovitch, C. Paur, S. Cundy, Q. Li, D. Calabro, *Chem. Commun.* **2012**, *48*, 4606-4608; b) W. Li, H. Shi, J. Zhang, *ChemPhysChem* **2014**, *15*, 1772-1778; c) Z. Xie, C. Wang, K. E. deKrafft, W. Lin, *J. Am. Chem. Soc.* **2011**, *133*, 2056-2059; d) J. X. Jiang, C. Wang, A. Laybourn, T. Hasell, R. Clowes, Z. Khimyak Yaroslav, J. Xiao, J. Higgins Simon, J. Adams Dave, I. Cooper Andrew, *Angew. Chem., Int. Ed.* **2010**, *50*, 1072-1075.

[37] P. Kaur, J. T. Hupp, S. T. Nguyen, *ACS Catal.* **2011**, *1*, 819-835.

[38] L. Ma, M. M. Wanderley, W. Lin, *ACS Catal.* **2011**, *1*, 691-697.

[39] L. Pop, F. Dumitru, N. D. Hădade, Y.-M. Legrand, A. van der Lee, M. Barboiu, I. Grosu, *Org. Lett.* **2015**, *17*, 3494-3497.

[40] J. C. Bertolini, P. Delichere, B. C. Khanra, J. Massardier, C. Noupa, B. Tardy, *Catal. Lett.* **1990**, *6*, 215-223.

[39] J. Chen, W. Zhang, L. Chen, L. Ma, H. Gao, T. Wang, *ChemPlusChem* **2012**, *78*, 142-148.

[41] V. I. Nefedov, Y. V. Salyn, I. I. Moiseev, A. P. Sadovskii, A. S. Berenbljum, A. G. Knizhnik, S. L. Mund, *Inorg. Chim. Acta* **1979**, *35*, L343-L344.

[43] F. Zhao, A. Vrajitoarea, Q. Jiang, X. Han, A. Chaudhary, J. O. Welch, R. B. Jackman, *Sci. Rep*. **2015**, *5*, 13771.

[44] A. Ganguly, S. Sharma, P. Papakonstantinou, J. Hamilton, *J. Phys. Chem. C* **2011**, *115*, 17009-17019.

[45] S.J. Pennycook, Ultramicroscopy **1989**, *30*, 58-69.

[46] J. M. Richardson, C. W. Jones, *J. Catal.* **2007**, *251*, 80-93.

[47] B. Elvers, S. Hawkins, W. Russell, in *Ullmann's Encyclopedia of Industrial Chemistry, Vol. vol. A 15*, VCH, New York **1990**, p. 91.

[48] a) Y. Wei, B. Rao, X. Cong, X. Zeng, *J. Am. Chem. Soc.* **2015**, *137*, 9250-9253; b) R. Noyori, T. Ohkuma, *Angew. Chem., Int. Ed.* **2001**, *40*, 40-73.

[49] a) F. Gao, A. D. Allian, H. Zhang, S. Cheng, M. Garland, *J. Catal.* **2006**, *241*, 189-199; b) Y. Gou, X. Liang, B. Chen, *Catal. Today* **2013**, *216*, 200-204; c) S.-i. Fujita, Y. Onodera, H. Yoshida, M. Arai, *Green Chem.* **2016**, *18*, 4934-4940; d) D. Duraczyńska, A. Drelinkiewicz, E. Bielańska, E. M. Serwicka, L. Lityńska-Dobrzyńska, *Catal. Lett.* **2011**, *141*, 83-94.

[50] A. Drelinkiewicza, A. Waksmundzka, W. Makowski, J. W. Sobczak, A. Król, A. Zieba, *Catal. Lett.* **2004**, *94*, 143-156.

[51] https://depts.washington.edu/eooptic/linkfiles/dielectric_chart%5B1%5D.pdf.

[52] H.E.B. Lempers, R.A. Sheldon, *J. Catal*. **1998,** *175***,** 62–69.